Electronic Supplementary Material (ESI) for ChemComm.


# Supplementary Information

## Geometry modulation of ion diffusion through layered asymmetric graphene oxide membranes

Jinlei Yang, Xiaopeng Zhang, Fengxiang Chen* and Lei Jiang

### Materials and Methods

Free-standing layered GO membranes (GOMs) were fabricated by drop-cast of GO colloids (~3.5 mg $ml^{-1}$, purity >98.5%, purchased from Nanjing 2DNANO Tech. Co., Ltd. (www. mukenano. com)) on cellulose acetate membranes (Whatman), following a previously reported procedure.[1] By changing the volume and inclination of GO solution, the different thickness gradient of the resulting membranes can be controlled with asymmetric ratio from ~1 to more than ~4. In this work, the thickness of the tested thin side of GOMs was kept at about 10 μm. After a mild thermal annealing process, the GOMs were highly stable in water.

**S1. Electrical measurement**

The piece of rectangular GO strip was embedded in a transparent polydimethylsiloxane (PDMS) elastomer (Scheme 1). The two sides of the sealed GOM were trimmed off to open the lateral ends of the membrane. A custom-made two-compartment electrochemical cell was then built on the two sides of the GO strip (Fig. S1). ~3.5 ml ionic solution with concentrations of KCl and deionized water was filled in each reservoir. Ag/AgCl electrodes were used to record the horizontal ion transport through the GOM. The electrical characteristics of the devices were measured using a Keithley 2636B source meter (Keithley Instruments). All measurements were performed at room temperature in air.

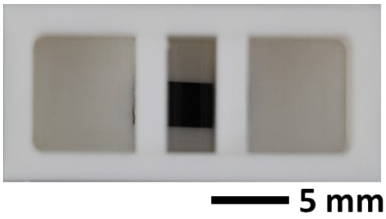


**Fig. S1** An optical image of the device of Teflon-structured two reservoirs. Ag/AgCl electrodes were used to investigate the horizontal ionic diffusion current through the PDMS sealed GOM.

**S2. XRD analysis**

X-ray diffraction tests were conducted on an X-ray diffractometer (Rigaku D/max 2500PC). After being soaked in water, the layered structure of GOM is well preserved, revealed by XRD analysis. The d-spacing increases from about ~0.77 to ~1.26 nm (Fig. S2a) due to the adsorption of additional water layers on GO sheets.[2] XRD patterns of the hydrated GOMs as a function of position are shown in Fig. S2b, indicating that the channel height remains uniform throughout the entire thickness gradient film.

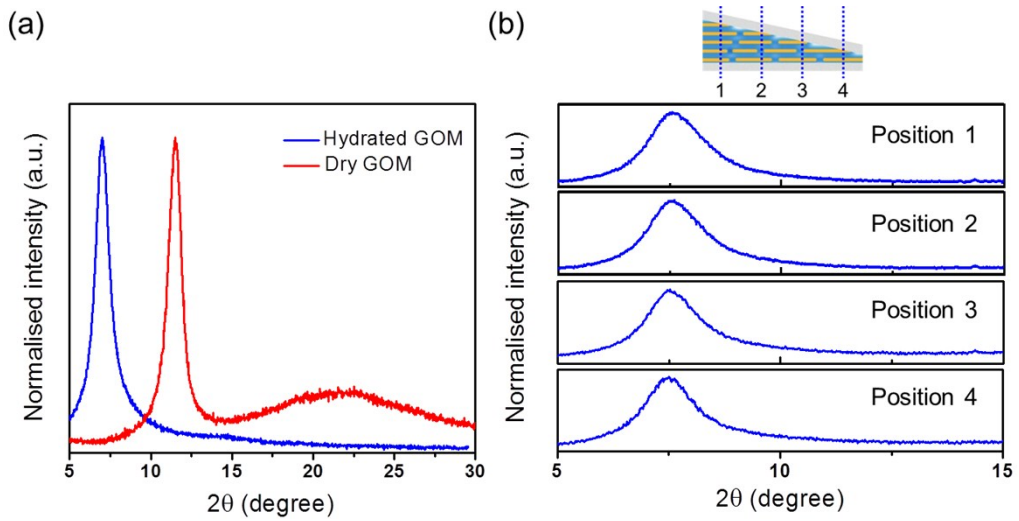


**Fig. S2** X-ray diffraction (XRD) patterns recorded on the GOMs. (a) XRD patterns on GOMs before and after being soaked in water. (b) XRD patterns of four different positions in a thickness gradient GOM with thick side of ~24 μm and thin side of ~11 μm.

**S3.FTIR spectrum**

FTIR spectrum (Bruker, TENSOR-27) was used to characterize the surface functional groups on GOM. Fig. S3 shows the band position corresponding to the functional groups, such as -OH (~3200 cm-1), C=O (1718 cm-1), C=C (1618 cm-1), and C-O-C (1045 cm-1), in the infrared spectra.[3]

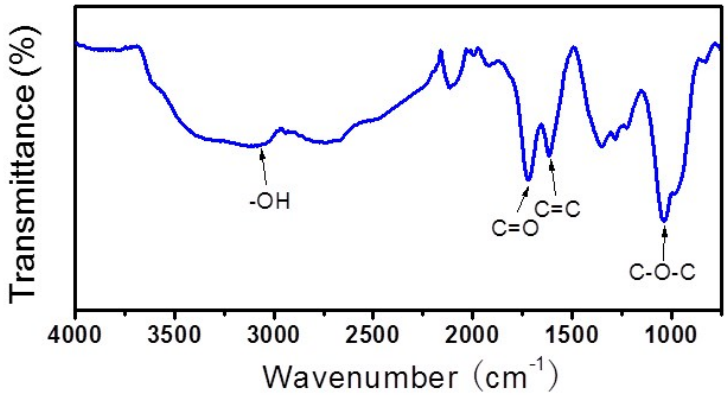


**Fig. S3** FTIR spectra of GOM.

**S4. Raman analysis**

Raman spectrum (Horiba, Labram HR Evolution) were used to determine the quality of the GOM in terms of defects or structural disorder, particularly focusing on the intensity ratio of D and G bands at ~1350 $cm^{-1}$ and ~1580 $cm^{-1}$ ($I_D/I_G$), respectively.[4] The D band arises from out-of-plane carbon vibrational mode and indicates defects or structural disorder in the materials, and the G band is associated with $sp^2$ in-plane vibrations. Therefore, a higher ratio of the intensities of D and G bands ($I_D/I_G$) implies in a higher $sp^3/sp^2$ ratio and an increase in the amount of defects/disorder on the graphene sheet. As shown in Fig. S4, $I_D/I_G$ can be identified of 0.96, which is comparable to the reported values of GO.[4, 5]

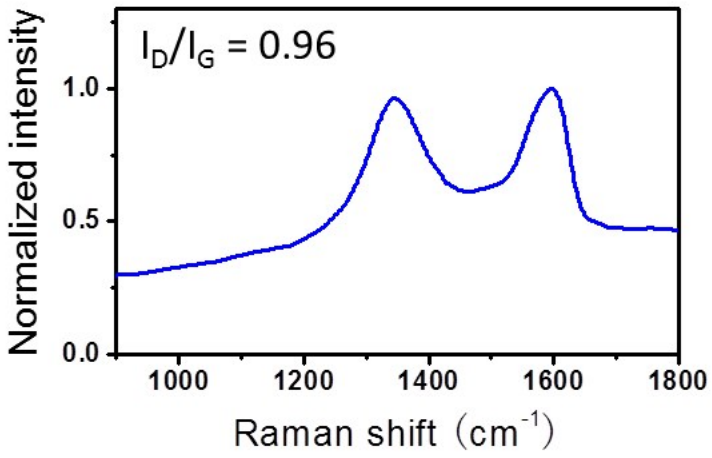


**Fig. S4** Raman Spectra of GOM. The defects or structural disorder was characterized by the intensity ratio of D and G peak ($I_D/I_G$).

**S5. Asymmetric diffusion current through the thickness gradient GOM**

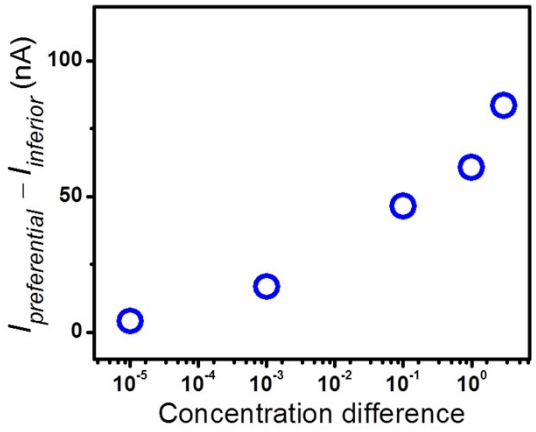


**Fig. S5** Comparison of the difference between $I_{preferential}$ (thick→thin) and $I_{inferior}$ (thin→thick) ($\Delta I_{\mathrm{diff}}$) for the thickness gradient GOM (24 μm:11 μm).

**S6. Cation transference number**

In the presence of transmembrane concentration difference, agar-saturated potassium chloride salt bridges were used to eliminate the imbalanced redox potential on the electrode|electrolyte interface. Ag/AgCl electrodes were used to record the current-voltage response. The two diffusion potentials from preferential direction and inferior direction were measured under different concentration gradients from 10 to $10^6$-fold (Fig. S6).

As mentioned in the main text, the cation transference number ($t_+$) quantifies the selective ion transportation. The value of $t_+$ can be calculated by[6]:

$$2t_+ - 1 = \frac{E_{Diff}}{\frac{RT}{zF}\ln(\frac{\gamma_{c_H} c_H}{\gamma_{c_L} c_L})}$$

where $R$, $T$, $z$, $F$, $\gamma$, $C_H$, and $C_L$ represent the gas constant, temperature, charge valent, Faraday constant, activity coefficient of ions, high and low ion concentrations, respectively. Since the decrease of the electric double layer in high salt electrolyte, both the membrane charge selectivity of $t_+$ in two directions show a decrease as a function of concentration gradient. However, due to the presence of negative surface charge on GO sheets and the extremely narrow channel width, the measured $t_+$ is all over 0.75.

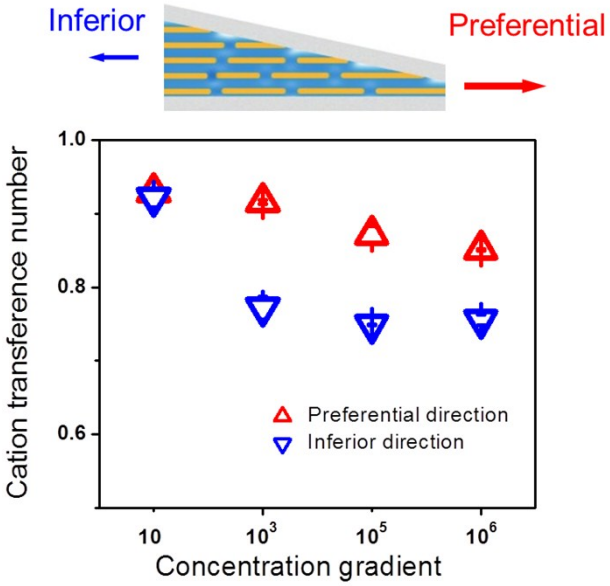


**Fig. S6** Cation transference number ($t_+$) of two diffusion directions measured under different concentration differences. KCl concentration in the low side was kept at 1μM.The geometry asymmetric ratio of the measured GOM is about 2.09.

**S7. Ion diffusion for different ionic species**

We investigated the ionic type dependence of the ion diffusion with many types of mono- and bivalent ions (Fig. S7). Although having larger hydration radius, the diffusion rate for bivalent ions can be as high as the monovalent ions.

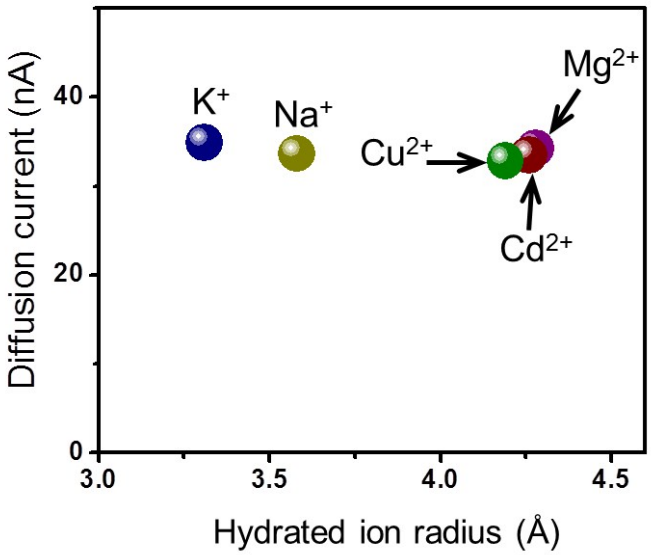


**Fig. S7** Concentration-driven ion diffusion for different ionic species. 1mM KCl ionic solutions and deionized water was filled in feed and permeate reservoirs, respectively. The geometry asymmetric ratio of the measured GOM is about 2.09. The diffusion current was characterized from the preferential direction (thick side→thin side).

**S8. Ion diffusion for different ionic species**

The surface charge property of the GOM was adjusted by the tuning the pH of the electrolyte solutions.[7] The feed KCl electrolyte solution was kept at 0.1 M. To avoid the interference of protons and metal ions brought by the acid or alkaline solution, the test was conducted in the pH range from 3.0 to 10.0. As shown in Fig. S8, the diffusion current roughly goes up with the pH. Enhanced surface charge density can promote the ion diffusion transfer rate.

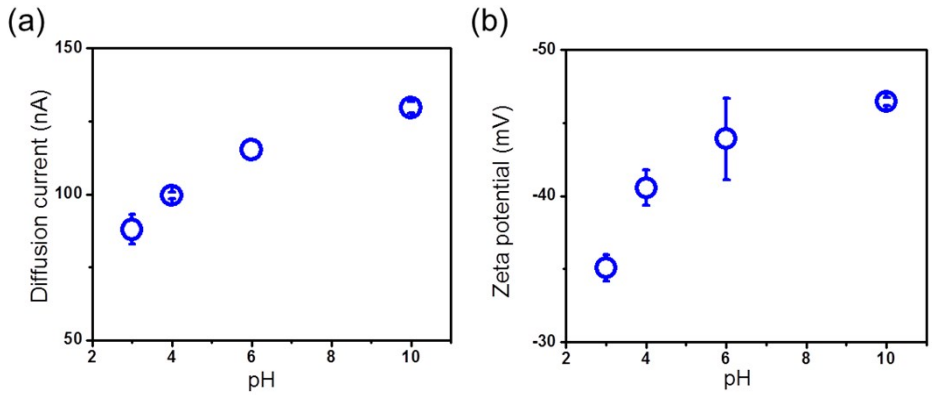


**Fig. S8** (a) Diffusion current measurements at varied pH. (b) Zeta potential measurements on GO colloids (0.1 mg/mL) at varied pH. The geometry asymmetric ratio of the measured GOM is about 2.09. The diffusion current was characterized from the preferential direction (thick side→thin side).

**S9. Current density ratio of the two opposite directions**

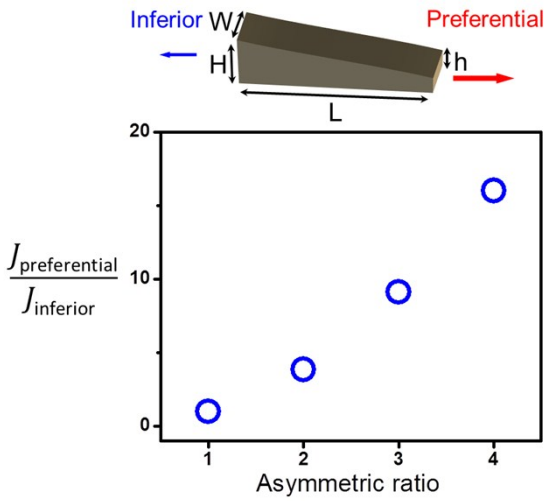


**Fig. S9** Current density ratio of the two opposite directions as a function of the asymmetric ratio. The active cross-sectional area of preferential outflow direction decreases sharply than that of inferior outflow direction with the asymmetric ratio.

**Table S1**. Summarized asymmetry ratio (H/h) and $\Delta I_{diff}$ of a series of thickness gradient GOMs. The feed KCl electrolyte solution was kept at 1 M.

| Asymmetry ratio (H/h) | 1.05 | 1.20 | 2.18 | 2.40 | 2.70 | 3.00 | 3.67 | 4.29 |
|---|---|---|---|---|---|---|---|---|
| $I_{preferential} - I_{inferior}$ (nA) | 27.26 | 32.57 | 60.78 | 72.91 | 92.00 | 113.58 | 127.67 | 137.10 |

## References


1. J. Ji, Q. Kang, Y. Zhou, Y. Feng, X. Chen, J. Yuan, W. Guo, Y. Wei and L. Jiang, *Adv Funct Mater*, 2017, **27**, 1603623.
2. P. C. R. K. Joshi, F. C. Wang, V. G. Kravets, Y. Su, I. V. Grigorieva, H. A. Wu, A. K . Geim, R. R. Nair, *Science*, 2014, **343**, 752-754.
3. S. Stankovich, R. D. Piner, S. T. Nguyen and R. S. Ruoff, *Carbon*, 2006, **44**, 3342-3347.
4. P. L. dos Santos, R. A. Timm, L. T. Kubota and J. A. Bonacin, *ChemistrySelect*, 2016, **1**, 1168-1175.
5. J. L. F. Zhao, X. Huang, X. Zou, G. Lu, P. Sun, S. Wu, W. Ai, M. Yi, X. Qi, L. and J. W. Xie, H. Zhang, W. Huang, *ACS Nano*, 2012, **6**, 3027-3033.
6. J. Gao, W. Guo, D. Feng, H. Wang, D. Zhao and L. Jiang, *Journal of the American Chemical Society*, 2014, **136**, 12265-12272.
7. D. Li, M. B. Muller, S. Gilje, R. B. Kaner and G. G. Wallace, *Nat Nanotechnol*, 2008, **3**, 101-105.